

High quality factor AlN nanocavities embedded in a photonic crystal waveguide

D. Sam-Giao, D. Néel, S. Sergent, B. Gayral, M. J. Rashid et al.

Citation: *Appl. Phys. Lett.* **100**, 191104 (2012); doi: 10.1063/1.4712590

View online: <http://dx.doi.org/10.1063/1.4712590>

View Table of Contents: <http://apl.aip.org/resource/1/APPLAB/v100/i19>

Published by the [American Institute of Physics](http://www.aip.org).

Related Articles

Thickness dependence of the amplified spontaneous emission threshold and operational stability in poly(9,9-dioctylfluorene) active waveguides

J. Appl. Phys. **111**, 093109 (2012)

Double embedded photonic crystals for extraction of guided light in light-emitting diodes

Appl. Phys. Lett. **100**, 171105 (2012)

Nonreciprocal optical Bloch-Zener oscillations in ternary parity-time-symmetric waveguide lattices

Appl. Phys. Lett. **100**, 151913 (2012)

Analysis of dielectric loaded surface plasmon waveguide structures: Transfer matrix method for plasmonic devices

J. Appl. Phys. **111**, 073108 (2012)

Coupling of energy from quantum emitters to the plasmonic mode of V groove waveguides: A numerical study

J. Appl. Phys. **111**, 064323 (2012)

Additional information on *Appl. Phys. Lett.*

Journal Homepage: <http://apl.aip.org/>

Journal Information: http://apl.aip.org/about/about_the_journal

Top downloads: http://apl.aip.org/features/most_downloaded

Information for Authors: <http://apl.aip.org/authors>

ADVERTISEMENT



GET YOUR COPY TODAY >>

**FREE CD with 700
Multiphysics Presentations**

COMSOL

High quality factor AlN nanocavities embedded in a photonic crystal waveguide

D. Sam-Giao,¹ D. Néel,² S. Sergent,³ B. Gayral,¹ M. J. Rashid,³ F. Semond,³ J. Y. Duboz,³ M. Mexis,⁴ T. Guillet,⁴ C. Brimont,⁴ S. David,² X. Checoury,² and P. Boucaud²

¹CEA-CNRS group "Nanophysique et semiconducteurs," INAC-SP2M, CEA-Grenoble, 17 rue des Martyrs, 38054 Grenoble Cedex 9, France

²Institut d'Électronique Fondamentale, UMR CNRS 8622, Université Paris Sud-11, F-91405 Orsay, France

³CRHEA-CNRS, Rue Bernard Grégory, 06560 Valbonne, France

⁴Université Montpellier 2, Laboratoire Charles Coulomb, CNRS UMR 5221, F-34095 Montpellier, France

(Received 16 March 2012; accepted 16 April 2012; published online 9 May 2012)

We present a spectroscopic study of nanocavities obtained by small modifications of a W1 waveguide in an AlN photonic crystal membrane. The AlN film containing GaN quantum dots is grown on silicon. The photonic crystal structure is defined by e-beam lithography and etched by inductively coupled plasma reactive ion etching, while the membrane is released by selective etching of the silicon substrate. The room temperature photoluminescence of the embedded quantum dots reveals the existence of even-symmetry and odd-symmetry confined cavity modes and guided modes. Cavity mode quality factors up to 4400 at 395 nm and 2300 at 358 nm are obtained. © 2012 American Institute of Physics. [<http://dx.doi.org/10.1063/1.4712590>]

Semiconductor microcavities with high quality factor (Q) resonances in the ultraviolet (UV) range will allow to seek original fundamental effects and applications in the field of optoelectronics. For emitters coupled to such a cavity in the weak coupling range, microlasing might well be a solution to obtain a compact semiconductor source at UV wavelengths (300–400 nm).¹ In the strong coupling regime, the large excitonic binding energy of excitons in wide bandgap semiconductors will allow for polariton lasing at room-temperature and large excitation densities.²

Compared to the III-As, III-P or Si systems in which extraordinarily large quality factors can be obtained thanks in particular to a mastering of the dry-etching process, it is much more challenging to process microcavities in III-N semiconductors because (1) these compounds are intrinsically more difficult to etch smoothly and (2) resonant structures in the UV are much smaller in size than similar structures resonant in the near infrared so that they are more sensitive to light scattering defects introduced during the process. Microdisk cavities and photonic crystal cavities have been fabricated at blue-violet wavelengths in the InGaN/GaN system with Qs up to 4000 in the case of microdisks^{3,4} while a Q of 5200 at 420 nm was recently reported for L7 cavities in a suspended photonic crystal membrane.⁵ The GaN/AlGaIn system allows to go further into the UV. In this system, Arita and coworkers demonstrated a Q of 2400 at 383 nm in an AlN photonic crystal membrane L7 cavity containing GaN quantum dots (QDs).⁶ In a similar system, Néel and coworkers demonstrated a Q of 1800 at 425 nm in a L3 cavity obtained by conformal growth on a patterned silicon substrate.⁷ Concerning microdisks, a Q of 7300 at 413 nm was demonstrated in a 5 μm diameter AlN microdisk containing GaN QDs.⁸ We study in the present article AlN nanocavities obtained by a small width modulation of photonic crystal W1 waveguide. We identify both confined modes and guided modes, with two families of modes: a low energy one is even with respect to the waveguide axis while

the high energy one is odd. Finally, we demonstrate at room temperature a record high Q of 4400 at 395 nm in such a low volume cavity at UV wavelength while a Q of 2300 is demonstrated at 358 nm.

The studied samples were grown on silicon (111) substrates by ammonia molecular beam epitaxy. A 35 nm-thick buffer layer of AlN is first grown on the Si substrate, followed by the growth of one plane of GaN QDs, which is then capped by 35 nm AlN.⁹ It has previously been shown that despite the thinness of the AlN buffer on the highly mismatched Si substrate, the GaN QDs luminesce efficiently, even at room temperature.⁹ A 100-nm thick silica layer is then deposited in order to be used as a hard mask for AlN etching. The silica layer is patterned by a 80 keV e-beam lithography followed by reactive ion etching. After cleaning of the resist residues, the pattern is transferred to AlN by chlorine-based inductively coupled plasma etching with Cl₂/Ar (20 sccm/5 sccm) gas. Finally, the membrane is released by selective etching of the Si substrate using XeF₂ gas (Figure 1). The growth of the nitride layer on a silicon

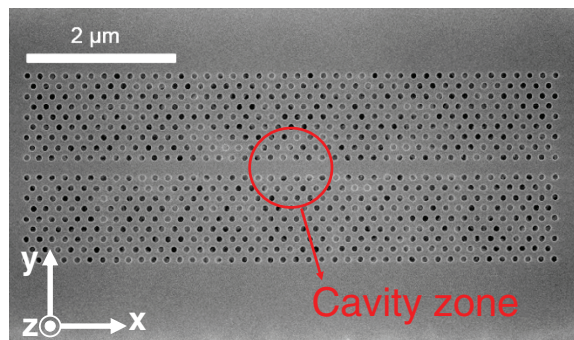


FIG. 1. Scanning electron micrograph of a typical AlN suspended photonic crystal structure including a waveguide structure. Parameters for this structure are $a = 170$ nm, $r = 42.5$ nm (filling factor 0.23). The small displacements ($d = 9$ nm) forming the cavity are not seen at this scale. The decreased contrast observed on some holes is an artifact due to the underetched silicon: the white residue is located microns below the membrane.

substrate has the advantage of making these structures potentially compatible with Si-based microelectronics for future integration and to ease the release of the photonic crystal membrane as highly selective etching processes between Si and III-N are available. This is in strong contrast with the complex process needed for selective removal of SiC (Ref. 6) or Al₂O₃ (Ref. 10) substrates.

Nanocavities were defined in W1 waveguides (Figure 1) by slightly displacing 30 holes away from the waveguide center, following a design proposed by Kuramochi and co-workers.¹¹ we used design A1 of their Figure 1, varying the displacement d (corresponding to d_A in Ref. 11) from 3 to 12 nm in steps of 3 nm. The lattice parameter a was set to 150 nm or 170 nm, while the ratio of the hole radius r to the lattice parameter a was either 0.25 or 0.27. The cavities were probed at room temperature by microphotoluminescence using a focused CW laser (spot size $\sim 1 \mu\text{m}$) at 244 nm (frequency doubled Ar laser) or 266 nm (Crylas/FQCW 266-50). The excitation laser was focused through a microscope objective (numerical aperture 0.4) on the center of the pattern (i.e., at the cavity location) and the photoluminescence (PL) was collected through the same objective. The PL signal was analyzed by a grating spectrometer with 550 mm focal length (1200 grooves mm^{-1} or 3600 grooves mm^{-1} gratings) and detected by an UV-enhanced liquid nitrogen cooled Si charge coupled device detector.

Figure 2 shows typical PL spectra of series of cavities with $a = 170 \text{ nm}$, $r = 46 \text{ nm}$, and varying d . All spectra show well-defined peaks distributed in two groups: a low energy group in the 3.19–3.25 eV range, and a high energy group in the 3.32–3.40 eV range. Such a wealth of spectral features has not been reported in the literature on similar cavities. Indeed, these cavities have so far been probed by transmission measurements with a focus on the confined

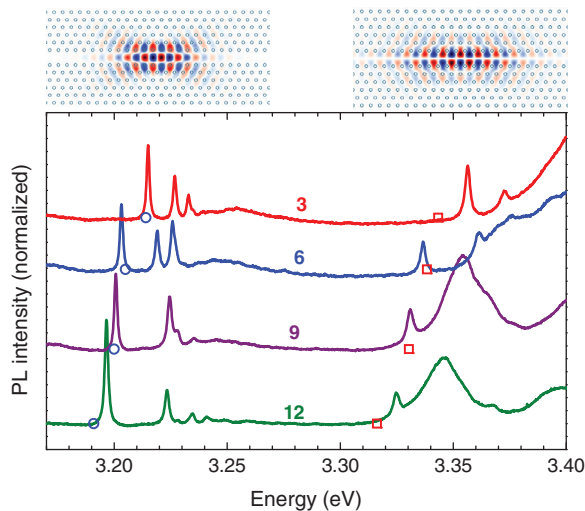


FIG. 2. Room temperature microphotoluminescence spectra of a series of cavities. Parameters are $a = 170 \text{ nm}$ and $r = 46 \text{ nm}$ ($r/a = 0.27$). Parameter d varies as indicated (in nm) on the figure. The GaN QD luminescence filtered by the photonic structure resonances gives rise to the peaks observed in the spectrum. The blue circles (respectively, red squares) indicate the position of the calculated low energy peaks of the low (respectively, high) energy group of peaks. The diagrams above the graph show 3D-FDTD simulations for the H_z component of the field of the even and odd confined cavity modes.

cavity mode (which in our case corresponds to the low energy peak of each group as analyzed hereafter). From Figure 2, it appears that the peaks follow a trend when d varies, for instance the lowest energy peak blue-shifts when d is reduced. In order to assign these peaks, we have performed 3D-FDTD simulations of the structure. In Figure 2, we indicate the calculated spectral positions of the lowest energy modes of each group of peaks. In the low energy group of peaks (around 3.2 eV), the numerical simulation shows that the low energy peak corresponds to a tightly confined mode in the cavity defined by the slight hole displacement at the waveguide center. The peaks at slightly larger energy (still in the low energy group) correspond to the fundamental guided mode of the W1 waveguide with even symmetry for the H_z or E_y field amplitude with respect to the waveguide axis. Interestingly, the high energy group of peaks (around 3.33 eV) also consists of a cavity mode and a guided mode, however, in that case with odd symmetry (see Figure 2), as also reported in Ref. 12. These modes are usually not seen in transmission experiments as the probe beam has even symmetry and thus only couples to the even symmetry fundamental mode of the waveguide. Both for even and odd modes, the theoretical trend when varying d follows the expected behavior: the guided modes shift only marginally when varying d as the cavities only weakly perturb the extended guided modes. The confined modes of the nanocavity shift to lower energy with respect to the guided mode when d is increased as the depth of this defect level increases.

When comparing the calculated absolute positions of the modes with the experimental data, Figure 2 shows that a good agreement is obtained for both the even cavity modes and the odd cavity modes. To be more quantitative, we have compared (Figure 3) simulation and experimental data in terms of splitting between the even cavity mode and the even guided mode, and between even and odd cavity modes. In that case, a good agreement is found between the calculation and the experimental spectra, thus giving confidence that the peak assignment is correct.

An important figure of merit for optical cavities is the quality factor. For the studied sample, quality factors in the 2000–4000 range were routinely measured for the even cavity resonance. The simulations indicate an intrinsic Q factor between $\sim 10\,000$ (for $d = 12 \text{ nm}$) and $20\,000$ (for $d = 3 \text{ nm}$) for the series presented in Figure 2. The experimental values for Q are thus still far from the theoretical maximum value. Reasons for that could be in residual absorption, scattering on process-induced defects, and deviations from the nominal design. We note that L3 cavities processed in the same conditions on the same sample exhibit much lower quality factors in the 1000–2000 range. As residual absorption would have a similar effect (or even larger) in waveguide cavities than in L3 cavities, the observed trend seems to indicate that residual absorption is not the dominant factor. It rather suggests that the waveguide cavities show more robustness with respect to processing defects than L3 cavities. On the other hand, waveguide cavities have a modal volume ($2.2 (\lambda/n)^3$) larger than that of L3 cavities ($0.8 (\lambda/n)^3$) so that both types of cavities in our sample have their own advantage for cavity quantum optoelectronics.

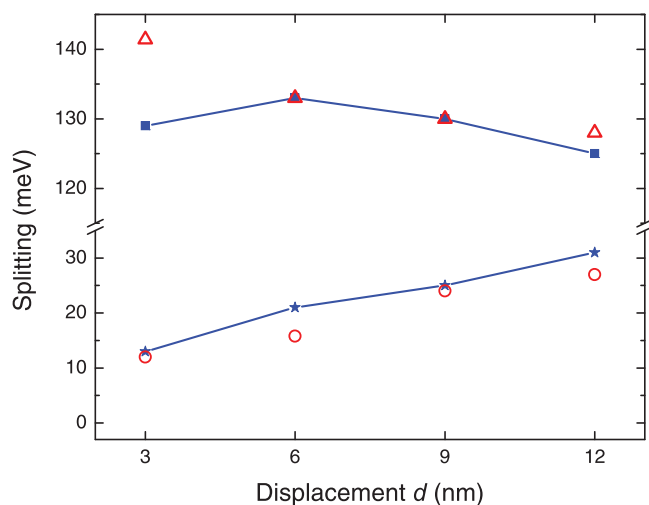


FIG. 3. Comparison of the experimental and theoretical values of the splitting between various resonances. Blue stars (respectively, red circles): theoretical (respectively, experimental) splitting between the even cavity mode and guided mode. Blue squares (respectively, red triangle): theoretical (respectively, experimental) splitting between the even and odd cavity modes. Lines are guides for the eyes.

Although the simulations predict a larger quality factor for width-modulated waveguide cavities with a small displacement d , we did not observe such a trend experimentally. This is not surprising as the experimentally measured Q is much lower than the theoretical limit, so that intrinsic photonic losses play a minor role in the experimental Q factor. It appears that a given cavity quality factor depends more on the slight variations of the process quality than on the cavity parameters. The largest measured Q factor is 4400 at 395 nm (Figure 4) for a cavity with $a = 170$ nm and $r = 0.27a$. This corresponds to a Purcell factor of 150. A general trend is that cavities resonating at shorter wavelengths (i.e., with $a = 150$ nm) tend to have smaller quality factors. We nonetheless could measure a quality factor of 2300 for a cavity resonating at 358 nm (Figure 4), which shows that small volume/large quality factor cavities can be fabricated and probed in the UV.

In conclusion, we have presented an optical study in the UV of high quality factor cavities designed as shallow defects in a photonic crystal waveguide. The comparison with theoretical calculations allows to identify confined and guided modes, both of even and odd symmetries with respect to the waveguide axis. While these nanocavities establish the state of the art for AlN based cavities resonating at UV wavelength, their processing can still be improved in order to approach the theoretical Q values. Interestingly, the resonant wavelength of the most UV cavity shown in Figure 4 is around the bandgap of GaN. This shows that the prospect of fabricating high quality photonic crystal for strong coupling with the bulk GaN exciton is realistic.

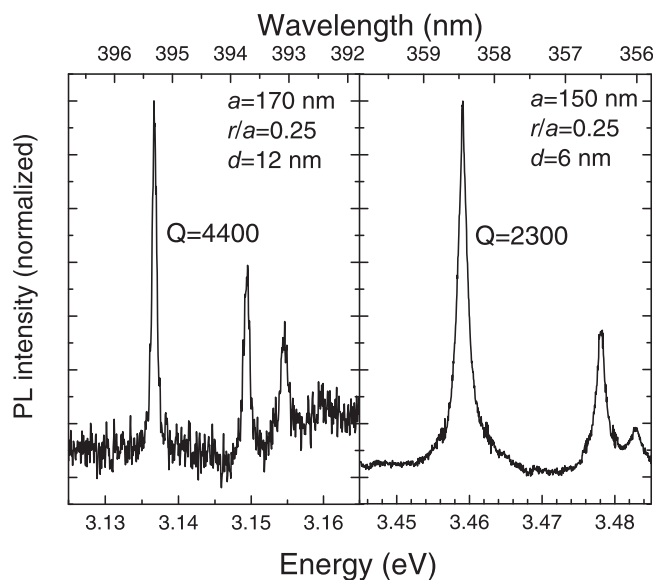


FIG. 4. Room temperature microphotoluminescence of high Q cavity modes for two width-modulated waveguide cavities.

This work has been supported by the French National Agency (ANR) in the frame of its program in Nanosciences and Nanotechnologies (SINPHONI Project No. ANR-08-NANO-021). M. Mexis acknowledges funding from the European project Clermont4 (FP7-PEOPLE-ITN-2008 235114).

- ¹Y. V. Radeonychev, I. V. Koryukin, and O. Kocharovskaya, *Laser Phys.* **19**, 1207 (2009).
- ²J. Kasprzak, M. Richard, S. Kundermann, A. Baas, P. Jeambrun, J. M. J. Keeling, F. M. Marchetti, M. H. Szymanska, R. André, J. L. Staehli, P. B. Littlewood, B. Deveaud, and Le Si Dang, *Nature (London)* **443**, 409 (2006).
- ³D. Simeonov, E. Feltn, H.-J. Bühlmann, T. Zhu, A. Castiglia, M. Mosca, J.-F. Carlin, R. Butté, and N. Grandjean, *Appl. Phys. Lett.* **90**, 061106 (2007).
- ⁴A. C. Tamboli, E. D. Haberer, R. Sharma, K. H. Lee, S. Nakamura, and E. L. Hu, *Nat. Photonics* **1**, 61 (2007).
- ⁵N. Vico Triviño, G. Rossbach, U. Dharanipathy, J. Levrat, A. Castiglia, J.-F. Carlin, K. A. Atlasov, R. Butté, R. Houdré, and N. Grandjean, *Appl. Phys. Lett.* **100**, 071103 (2012).
- ⁶M. Arita, S. Ishida, S. Kako, S. Iwamoto, and Y. Arakawa, *Appl. Phys. Lett.* **91**, 051106 (2007).
- ⁷D. Néel, S. Sergent, M. Mexis, D. Sam-Giao, T. Guillet, C. Brimont, T. Bretagnon, F. Semond, B. Gayral, S. David, X. Chécoury, and P. Boucaud, *Appl. Phys. Lett.* **98**, 261106 (2011).
- ⁸M. Mexis, S. Sergent, T. Guillet, C. Brimont, T. Bretagnon, B. Gil, F. Semond, M. Leroux, D. Néel, S. David, X. Chécoury, and P. Boucaud, *Opt. Lett.* **36**, 2203 (2011).
- ⁹S. Sergent, J.-C. Moreno, E. Frayssinet, S. Chenot, M. Leroux, and F. Semond, *Appl. Phys. Express* **2**, 051003 (2009).
- ¹⁰C.-H. Lin, J.-Y. Wang, C.-Y. Chen, K.-C. Shen, D.-M. Yeh, Y.-W. Kiang, and C. C. Yang, *Nanotechnology* **22**, 025201 (2011).
- ¹¹E. Kuramochi, M. Notomi, S. Mitsugi, A. Shinya, and T. Tanabe, *Appl. Phys. Lett.* **88**, 041112 (2006).
- ¹²W. C. Stumpf, M. Fujita, M. Yamaguchi, T. Asano, and S. Noda, *Appl. Phys. Lett.* **90**, 231101 (2007).